MethodsX 7 (2020) 100742

Contents lists available at ScienceDirect

MethodsX

journal homepage: www.elsevier.com/locate/mex

Method Article

Automated rapid & intelligent microplastics mapping by FTIR microscopy: A Python–based workflow

Gerrit Renner[a,b,*], Torsten C. Schmidt[b], Jürgen Schram[a]

[a] Instrumental Analytical and EnvironmentalChemistry, Faculty of Chemistry, Niederrhein University of Applied Sciences, Frankenring 20, D-47798, Krefeld, Germany
[b] Instrumental Analytical Chemistry and Centre for Water and Environmental Research (ZWU), University of Duisburg-Essen, Universitätsstr. 5, D-45141, Essen, Germany

A B S T R A C T

The analysis of environmental microplastic particles using FTIR microscopy is a challenging task, due to the very high number of individual particles within a single sample. Therefore, automatable, fast and robust approaches are highly requested. Micro particles were commonly enriched on filters, and sub- or the whole filter area was investigated, which took more than 20h and produced millions of data, which had to be evaluated. This paper presents a new approach of such filter area analysis using an intelligent algorithm to measure only those spots on a filter that would produce evaluable FTIR data. Empty spaces or IR absorbers like carbon black particles were not measured which successfully reduced the total analysis time from 50h to 7h. The presented method is based on system independent Python workflow and can easily be implemented on other FTIR systems.

- *Fast and intelligent FTIR microscopy area mapping without FPA detector*
- *Total time reduction from 50 h to 7 h*
- *Platform independent approach based on Python*

A R T I C L E I N F O
Keywords: Microplasitcs, Mapping, Python, FTIR microscopy, Chemometrics
Article history: Received 3 October 2019; Accepted 14 November 2019; Available online 13 December 2019

* Corresponding author at: Instrumental Analytical and Environmental Chemistry, Faculty of Chemistry, Niederrhein University of Applied Sciences, Frankenring 20, D-47798, Krefeld, Germany.
E-mail addresses: grenner87@gmail.com (G. Renner), torsten.schmidt@uni-due.de (T.C. Schmidt), juergen.schram@hs-niederrhein.de (J. Schram).

https://doi.org/10.1016/j.mex.2019.11.015

Specification Table

Subject Area:	*Chemistry, direct submision*
More specific subject area:	*Describe narrower subject area*
Method name:	*Rapid and intelligent microplastics mapping (μMAP)*
Name and reference of original method:	*Chemical Imaging by FTIR Microscopy*
Resource availability:	*Python:* https://www.python.org/downloads/

Introduction

Over the last years, analysis of microplastics shifted more and more from fragments >500 μm to real micro particles with diameters <100 μm [1,2]. In this context, microplastics were pre–separated from most matrix components [3–6] and transferred onto fine filter materials [7,8] for further analysis. Along with the decreasing size, the number of particles increased exponentially, which led to a high sample throughput task [9]. However, most established analysis methods to identify microplastics <100 μm are Fourier Transform Infrared microscopy (μFTIR) and Raman microscopy (μRaman), and both techniques conventionally analyze every particle individually [1,9,10]. Although single measurements are very fast, the total measurement time of a whole sample of micro particles, which are typically collected on a filter, is often greater than 20 h [11–14].

In general, there exist two approaches to analyze microplastics on filter materials, either to measure the complete filter area spot by spot [11–13], or to measure selected points of interest [15,16]. The first approach ensures that no particle is overseen. However, the maximum number of spots are investigated, which increases measurement time and produces big data that have to be evaluated [11,17]. Moreover, this approach cannot be recommended without using a focal plane array detector (FPA) or an electron–multiplying charge–coupled device (EMCCD), which allow to measure multiple spots (almost) simultaneously, as otherwise measurement time will be even longer.

The second approach reduces the number of spots and measurement time significantly and does not require an FPA detector [15]. However, there is an additional time–consuming step required to define points of interest, and furthermore, there is a risk of overlooking microplastic particles. Nevertheless, this approach saves analysis time considering that commonly only 1–10 % of the whole filter material is covered by micro–sized particles [11].

One already established technique to highlight interesting spots on filter materials is based on Nile Red that can be used as a characteristic marker for microplastics [15]. However, this approach needs special modifications to the microscope, e.g., an additional light source (450–510 nm) and an orange filter (529 nm) which lowers the practicability.

Within this report, a new alternative method to preliminarily detect microplastics with μFTIR will be presented. In contrast to the Nile Red technique, which uses an additional detection system for visible light, the main idea of the new method is to use the infrared spectrum directly to preliminarily detect microplastics. Therefore, a practical and manufacturer-independent concept will be described that uses a very fast single scan infrared spectrum (≈100 ms) of a discrete spot on the sample carrier to decide almost in real time whether to start a more accurate measurement with accumulated scan repetitions for further microplastics identification or to move on to the next spot. This approach ensures that every spot is investigated but only interesting points are measured in detail by accumulated FTIR scans, which reduces total measurement time significantly without losing relevant information.

Method details

Samples & references

For method development artificial micro particle / fiber mixtures of polyethylene (PE), polypropylene (PP), polyamide (PA), polyvinyl chloride (PVC), polystyrene (PS), polyethylene terephthalate (PET), sand and algae were examined. In total, three different model samples were

examined. Micro particle mixtures (Ia) and (Ib) had equal compositions to investigate the mapping repeatability, and a micro particle / fiber mixture (II) was analyzed to study microfiber detection. The detailed sample compositions can be found in Table S1. Every sample was randomly placed on a plane and reflecting surface of a sample carrier within an area of $10 \times 10\text{mm}^2$ for μFTIR analysis. In this context, the platter of a conventional hard disk was used as sample carrier due to its very precise and well-defined surface. Alternatively, any kind of plane mirror could be used for this mapping approach.

Measurement setup

All μFTIR measurements were performed in transflection mode on an IRTracer–100 IR spectrometer coupled with an AIM–9000 IR microscope from Shimadzu, which is equipped with a liquid nitrogen cooled MCT detector. In total, the analysis of an individual sample (up to $10 \times 10\ \text{mm}^2$) was divided into a regular grid of up to 40,000 spots (200×200). This results in a spatial resolution of $50 \times 50\ \mu\text{m}^2$. The spectral resolution was set to $16\ \text{cm}^{-1}$ while the mirror speed was increased to 0.582 cm/s, which reduced the measurement time of a single spectrum scan down to 107 ms. For the μFTIR analysis two different measurement techniques were used. Every spot was investigated by a single scan spectrum using a continuously and temporarily saved on-line monitor feature of the FTIR microscope. Every spot that contained a micro particle was additionally measured with 20 accumulating scans and stored for further data evaluation.

Identification of microplastics

All recorded IR spectra were automatically evaluated by the modified microplastics identification algorithm ($\mu\text{IDENT}_{\text{mod}}$) [18,19]. To validate the individual identification results, 500 randomly chosen spectra were evaluated by manual spectra inspection, in parallel to other studies [18,19].

Used software

The FTIR microscope was controlled by AIM Solution Measurement (Version 1.1.2). This software has two essential features for the presented mapping approach implemented: (1) Online FTIR Monitor allows to measure and plot FTIR single scans continuously. (2) XYZ-Stage Control allows to move the sample table of the microscope electronically via software. Both features are common for modern FTIR microscopes.

The automation of the developed mapping approach was realized by an in–house script based on Python 3.6 called μMAP that controlled the PC including the μFTIR software and evaluated the on-line IR spectra in real–time. The source code is attached to the Supporting Information and is free for use.

Development of a smart mapping approach

The main concept of the presented mapping approach is to move the sample stage of the μFTIR along a pre-defined grid within the measurement area step by step. While moving, the on-line FTIR monitor of the μFTIR software plots continuously the current FTIR spectrum of the investigated spot. This fast updated FTIR single scan signal was evaluated in real time to decide automatically if the current position should be held to start an accumulated permanently stored μFTIR measurement for further spectra evaluation. Otherwise the sample stage was moved further, which was the case, if the current spot was not interesting, e.g., the spot was empty or showed a non–evaluable FTIR spectrum. As a consequence, the analysis time can be significantly reduced for two reasons. (1) All empty or non–interesting spots were investigated only with a single instead of 20 accumulated scans. (2) Only FTIR spectra of interesting spots were stored for further data evaluation. Mathematically, the time saving factor f can be estimated by Eq. (1).

$$f = \frac{t_{move} + t_{meas} + t_{eval}}{t_{move} + (t_{maes} + t_{eval}) \cdot \chi} = \begin{cases} 1 & if \ \ \chi = 1 \\ 1 + (t_{maes} + t_{eval}) \cdot t_{move}^{-1} & if \ \ \chi = 0 \end{cases} \tag{1}$$

Where $t_{move,\ meas\ \&\ eval}$ are the time periods that are needed to move the sample stage to the next spot, measure the spot and evaluate the FTIR spectrum. Moreover, χ describes the degree of coverage of the sample carrier with microplastics. For the used setup $t = (0.34\ s, 2\ s, 2\ s)$ and $\chi = 0.05–0.10$, the time saving factor f ranges from 8 to 6.

How to distinguish between interesting & non–interesting spots

An essential step of this work was the development of a robust and practical decision criterion that allowed to distinguish between evaluable and non–evaluable data based on a single scan μFTIR spectrum. In this context, evaluable meant to be able to perform a reference spectra library search with the $\mu IDENT_{mod}$ algorithm [19], which compares the characteristic vibrational bands pattern of μFTIR spectra [19]. If the measured data only contained noise, the spectrum was defined as non–evaluable and no further accumulated scans were necessary. To that end, the signal–to–noise ratio (s/n) of the spectrum was used as decision criterion. For automation, a decision criterion ι was defined by Eq. (2), which can be deduced from s/n estimations.

$$\iota = \overline{Q_{90\%}}(|\delta A/\delta \sim \nu|) \tag{2}$$

Where $\overline{Q_{90\%}}(|\delta A/\delta \sim \nu|)$ describes the mean of the highest 10 % of the differentiated absorbance values within an FTIR spectrum and characterizes the signal quality. The sharper and more intense vibrational bands are, the higher the differential term will be.

To define a ι threshold for evaluable data, spectra of 1000 empty spots (non–evaluable class) and 300 microplastics of PE, PP, PA, PS and PVC (evaluable class) were evaluated as described in Eq. (2). Both data sets showed significantly different means (*t*-Test: $p < 0.05$) and the threshold was defined by a type 1 error of 0.1 % according to the evaluable class. Under these conditions, 0.04 % of the non–evaluable class were wrongly assigned to the evaluable class. Respecting this definition, the ι threshold was set to 0.015 for the used measurement setup. The experimental data of the threshold experiment is shown in Fig. S2.

Real–time evaluation of the μFTIR online plot

The great challenge of the new mapping approach is a real–time evaluation of the online FTIR signal using the decision criterion presented in Eq. (2). The online FTIR spectrum had to be transferred to Python, but unfortunately, the FTIR online monitor was only stored temporarily and the numeric data was encrypted, which denied a direct data export. This is common for measurement systems of most companies and had to be overcome somehow. However, the decision whether the μFTIR spectrum of the current spot is evaluable or not does not require highest spectra precisions. Therefore, a gray scale screen–shot from the online plot was taken by using the PIL.ImageGrab package for Python [20]. This image was stored as a numeric matrix B that contained brightness values (from 0 → black to 255 → white) and was transferred into data vectors that contained absorbance and wavenumber information. For this step, the position of the plotted black line was identified within the image matrix B. That was possible due to the very high contrast between the white background and black plot line. It was looked for all row indices i in every column that contained the minimum brightness value. This process is illustrated in Fig. 1.

The row indices i were stored in a vector $\vec{i}$, which is very similar to the absorbance vector of a measured μFTIR spectrum except for the value scaling. However, $\vec{i}$ was re–scaled by optical character recognition (OCR) of the x and y tick labels, which were also stored in separated matrices. By extracting these values and determining the tick positions, the step–widths Δx and Δy can be calculated by Eq. (3).

$$\Delta x, y = \frac{highest\ \ tick\ \ value - lowest\ \ tick\ \ value}{highest\ \ tick\ \ position - lowest\ \ tick\ \ position} \tag{3}$$

If the absorbance scaling ranges from 0.1 to 0.4 and the first and last ticks are separated by 600 pixels, every pixel or data point describes an absorbance difference Δa of 0.0005. The calculated

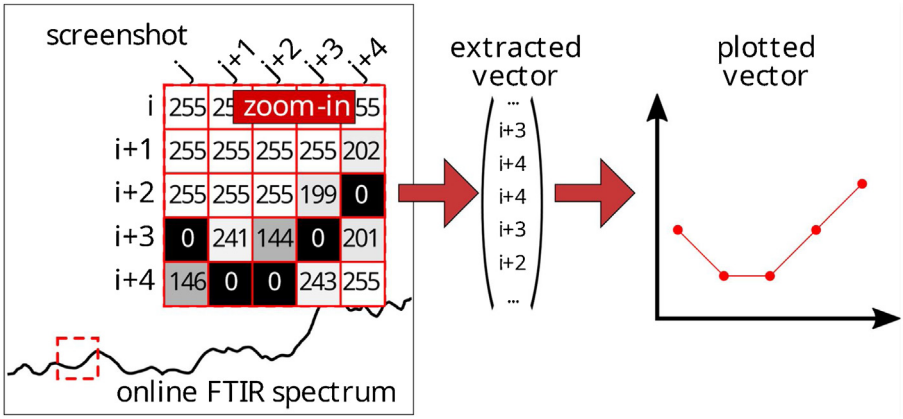

Fig. 1. Schematic workflow to extract the numeric spectral data from a screenshot of a plotted FTIR spectrum. Each pixel is a member of an n × m matrix and contains a gray scaled value. The line of the plotted spectrum is black and can be extracted by looking for the lowest gray scaled values within every column. The corresponding row indices correlate with the absorbance values of the original FTIR spectrum.

Δa was used as a correction factor and the minimum tick value was added as offset. Analogously, this procedure can be used to create the wavenumber vector.

For validation, the described data extraction protocol was applied on real measured μFTIR spectra. A comparison of extracted and measured μFTIR spectra showed very good matches with a $\overline{R^2}$ = 0:998 and $\overline{RMSE}$ = 0:04, which can be inferred from Fig. S1.

Controlling the μFTIR via Python

The μFTIR is commonly controlled by the μFTIR software from the manufacturer. This software contains all basic operations that are needed for the new automated microplastics mapping approach (μMAP). In detail the following operations were required:

- Start Measurement (Sample, Background & Online–Monitor)
- Move Sample Stage

A practical way to control the μ FTIR via Python is given by the win32api and win32con packages [21]. These allow Python to perform keyboard or mouse inputs and start, close and switch between other software applications. That means, the μ FTIR was controlled not directly but indirectly by recording and running keyboard and mouse macros by Python. To that end, two basic functions could be defined that are shown in Algorithm 1.

Algorithm 1 Basic Functions For Automation

```
function MOUSE_CLICK(x,y,t)
···| click mouse button at (x,y) for t seconds
function KEYBOARD_INPUT(k)
···| press key: k
```

Where x,y were pixel coordinates on screen, t was the elapsed time until releasing the mouse button and k was any key on the keyboard.

Following the idea of indirect control makes the presented method easier to implement on different μFTIR systems, as there is no advanced system specific knowledge needed, how to control the μFTIR directly via Python.

Defining the sample stage moving path

The simplest and most common measurement area is given by a rectangle or square, e.g., $10 \times 10\,mm^2$. For analysis, this area type was subdivided into a regular seamless grid of individual measurement spots ($100 \times 100\,\mu m^2$). The spots were positioned with 50 % overlapping each other to handle light diffraction based intensity attenuations at the edges of each spot. Otherwise blind spots could appear with the risk of overlooking microplastics. In concrete terms, the measurement area consisted of 40,000 individual spots within 200 rows and columns with an effective spatial resolution of 50 μ m. For automated mapping, the whole area was investigated row by row and column by column. If a spot showed any kind of evaluable μ FTIR spectrum, an accumulated measurement was initiated. Otherwise, the sample stage moved further. Respecting these steps, the following pseudo–code was defined (Algorithm 2). In this context, a time resolved process chart can be seen in Fig. S4.

Algorithm 2 Sample Stage Moving Path

```
for each row in the measurement area do
···| set x position of sample stage to 0 µm
···| for each column in the measurement area do
·····| move x position of sample stage 50 µm to the right
·····| get the decision criterion from the online monitor
·····| if decision criterion > threshold then
·····| measure µFTIR spectrum
·····| end if
···| end for
···| move y position of the sample stage 50 µm downwards
end for
```

The sample stage of the used μ FTIR was controlled by four direction buttons and the longer the buttons were pressed the further the sample stage was moved. A calibration experiment was performed by varying the moving time and measuring the corresponding traveled distance. Based on these data, which can be seen in Fig. S3, the sample stage moved 50 μm in 339 ms. Therefore, the move command from Algorithm 2 can be realized by the mouse_click basic function from Algorithm 1, which is contributed in Algorithm 3.

Algorithm 3 Move One Step Further

```
function MOUSE_CLICK_MOVE_SAMPLE_STAGE(x,y,t)
···| set x and y to coordinates of the direction button
···| set t to 339 milliseconds
···| click at (x,y) AND release the mouse button after t milliseconds
```

The actual moved mean distance differed slightly from 50 μm and was 49 ± 3 μm, and therefore, we decided to store the definite sample stage positions from the μFTIR software for further

corrections. In detail, the image section that contained the sample stage position was analyzed by OCR using the pytesseract package for Python [22].

Creating a false–color image of the complete measurement area

The presented mapping approach automatically investigated a pre–defined area and measured μFTIR spectra, if any kind of evaluable μFTIR spectrum was obtained at a specific spot (Algorithm 2). Additionally, an optical camera took images of each spot, which were stored and merged to a single photo of the whole area. This merging was also realized by Python. However, it had to be considered that the investigated spots overlapped each other, and therefore, the overlapping data from the optical images were merged with a Gaussian mixing gradient, which can be seen in Fig. 2. The mixing gradient matrix **G** was defined as follows in Eq. (4).

$$G = \frac{exp\left[\left(2\vec{w} + \vec{h}\right) \cdot a\right]}{(exp[\vec{w} \cdot a] + 1)\left(exp\left[\vec{h} \cdot a\right] + 1\right)} \quad , with \;\; a = 0.1 \cdot width \;\; of \;\; the \;\; photo \tag{4}$$

Where the $\vec{w}$,$\vec{h}$ are linear spaced perpendicular vectors from [$-0.5 \cdot$ size of the photo : $1.5 \cdot$ size of the photo].

The merged overview photos were used as background image for false–coloring, and different colors were connected to different assigned polymers after all measured μFTIR spectra were automatically evaluated by the $\mu IDENT_{mod}$ library searching algorithm [19]. In detail, the overview images were merged photo by photo and at the end of this process an optical particle recognition algorithm based on the opencv [23] package for Python was performed, which can be seen in Fig. 3. The black–white images from the particle recognition (Fig. 3b) were virtually subdivided into their origin tiles (Fig. 3c). Afterwards, all stored FTIR spectra were assigned to the detected particles. The particles were re–colored based on the identification results of their assigned FTIR spectra (Fig. 3d). If multiple spectra were linked to one particle, the most common identification result was applied first, followed by the highest Hit Quality Index. The false coloring can be obtained from Algorithm 4.

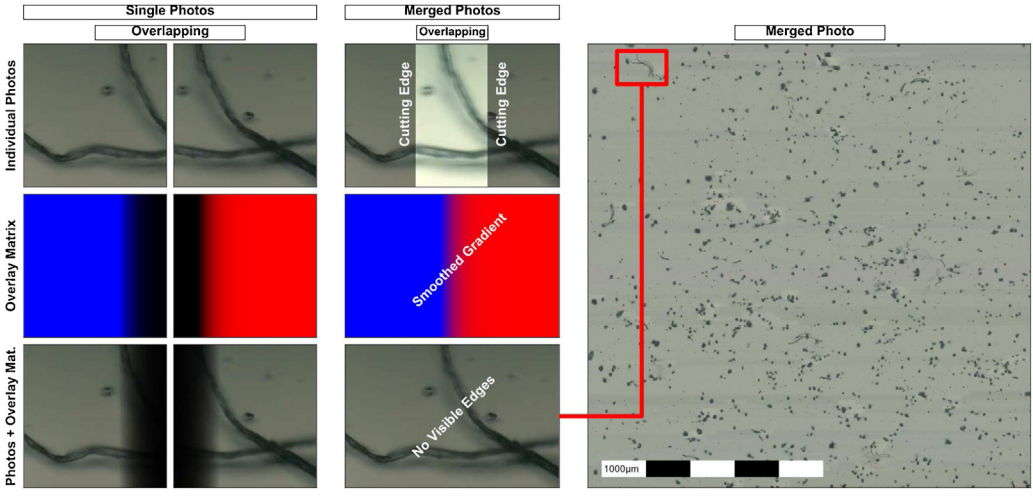

Fig. 2. The overviewing camera image of the mapped area consists of 40,000 individual overlapping photos. These were merged using a Gaussian gradient to avoid visible cutting edges.

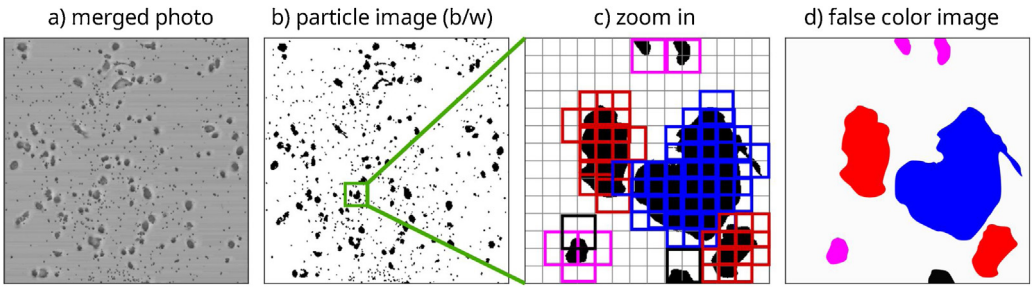

Fig. 3. The individual photos were merged together, and an optical particle recognition was performed. All measured FTIR spectra were assigned to the detected particles, while each FTIR spectrum covered four tiles, due to the overlapping measurements. The false coloring of each particle was based on the most common identification results of the FTIR spectra.

Algorithm 4 False-Coloring

```
do particle recognition on merged photo to get all particles
   and a black-white image
subdivide the black-white image into tiles
for each particle of all particles do
···| if there exists FTIR data then
·····| evaluate all FTIR spectra using µIDENT
·····| if there exists multiple results then
·····| get color based on highest Hit Quality Index
·····| end if
···| else
·····| get color based on the assignment result
···| end if
···| re-colorize particle within the black-white image
···| click at (x,y) AND release the mouse button after t milliseconds
```

Examination of µMAP with microplastics samples

The presented mapping approach was applied on three model samples, which consisted of diverse microplastics/matrix mixtures. According to Eq. (1) and the used parameter settings, an average time saving factor f = 7.3 for all mapping experiments could be achieved. A conventional spot by spot mapping of 40,000 spots including data evaluation would take ≈50 h but using the new µMAP approach reduced the analysis time down to ≈7 h, which increases practicability of mapping microplastics without an FPA detector significantly.

The individual results for all three mappings can be inferred from Fig. 4 and Table 1. In this context, all detected particles were identified automatically using the µIDENT mod algorithm [19]. For validation of the used library searching algorithm, 500 randomly chosen spectra were evaluated by manual spectra inspection. In total, 98.2 % of the identification results could be confirmed. Additionally, the equivalent circle diameter (ECD) [24] (particle size parameter) and the circularity [25] (particle shape parameter) were calculated from the false color images for each particle for further morphological characterization.

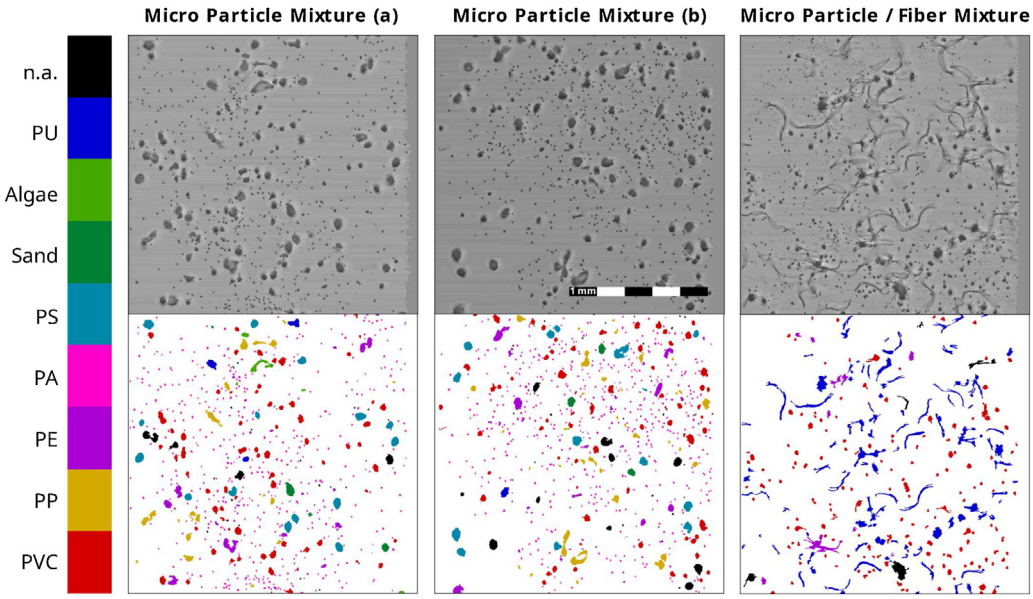

Fig. 4. Overview of the three mapped microplastics samples.

Table 1
Details of the mapping results.

	PE	PP	PS	PA	PVC	PU	Sand	Algae
	Ia) Micro Particle Mixture (n = 639)							
No. [%]	3.0	2.8	2.3	74.5	10.3	0.5	0.8	0.8
[a]ECD_{d50} [μm]	103	178	281	55	153	293	129	131
[a]$ECD_{d10,\ d90}$ [μm]	83, 300	85, 309	214, 305	46, 67	109, 224	215, 300	83, 310	95, 290
$Circularatiy_{d10,\ d90}$ [μm]	46, 89	39, 84	65, 81	79, 90	67, 85	64, 82	62, 83	45, 80
	Ib) Micro Particle Mixture (n = 715)							
No. [%]	3.5	4.9	2.0	72.9	9.5	0.1	0.4	
[a]ECD_{d50} [μm]	110	114	279	56	156	285	273	
[a]$ECD_{d10,\ d90}$ [μm]	88, 294	81, 279	212, 335	45, 67	97, 223	285, 285	248, 282	
$Circularatiy_{d10,\ d90}$ [μm]	56, 82	54, 81	56, 79	79, 90	69, 86	64, 64	69, 79	
	II) Micro Particle/Fiber Mixture (n = 263)							
No. [%]	3.4				58.2	36.5		
[a]ECD_{d50} [μm]	161				100	185		
[a]$ECD_{d10,\ d90}$ [μm]	121, 351				84, 160	102, 318		
$Circularatiy_{d10,\ d90}$ [μm]	24, 62				62, 86	26, 60		

[a] ECD: equivalent circle diameter; d10: 10 % percentile.

The measured sample compositions from (Ia, Ib) micro particle mixtures did not differ significantly ($\Delta < 5\,\%$), which indicates the repeatability of this new mapping approach. The equivalent circle diameters ranged from 50 to 300 μm. From Table 1 it could be inferred that the particle size distribution of polyamide was very close to its median ECD of 55 ± 10 μm, which agrees well with the manufacturer's specifications (50 ± 20 μm). For the other materials, there were no comparable data available and a particle size determination was not performed, as this was not the focus of the automated microplastics mapping approach.

The presented new method is suitable for microfiber detection as well, which can be deduced from the (II) micro particle / fiber mixture results in Table 1. In this case, polyurethane and polyethylene

micro fibers were mixed together with polyvinyl chloride micro spherules. Based on material and morphological aspects from IR spectroscopy and the optical microscope camera, there was a clear division into two groups, as expected. This can also be obtained from Fig. S5, where circularities and equivalent circle diameters from this sample are plotted against each other.

Conclusion

The new automated microplastics mapping approach μMAP is based on Python and can easily be transferred to all kinds of FTIR microscopes that can be controlled by a personal computer. The concept of using an online fast single IR scan to decide whether to start an accumulated measurement or keep moving to the next spot is a potential tool to reduce the measurement time of a microplastics mapping experiment. All spots are investigated with a 50 % overlapped measurement window to avoid overseeing microplastics. The recommended particle sizes range between 50−300 μm. The sample stage moved only along x– and y–axis, which limits this mapping approach to flat samples. However, an automatic z–axis compensation could be implemented by using the contrast information of the optical camera combined with the online FTIR monitor. The latter would show the best signal quality, if the sample surface is located in the focus plane of the FTIR microscope. In few cases, microparticles of carbon black were measured due to unusually high distinction criteria values. Therefore, it can be considered to implement a secondary threshold value to delimit upper extreme values.

The current μMAP approach uses discrete steps for sample stage movement. However, considering the FTIR scanning time of 107 ms and the moving speed of ≈ 400 μm/s, it should be possible to realize a continuously moving workflow, which could further increase the time saving factor up to ≈34, due to the elimination of the sample stage moving delay time. The time saving can be used to increase the spatial resolution. However, this would require deep modifications of the measurement system, because the sample stage moving speed and the sampling rate of the FTIR online monitor have to be customized. In this context, the sampling rate is the bottle neck, and therefore, spatial resolutions are limited to 25 μm for the μFTIR used in this study.

Declaration of Competing Interest

The authors declare that they have no known competing financial interests or personal relationships that could have appeared to influence the work reported in this paper.

Appendix A. Supplementary data

Supplementary material related to this article can be found, in the online version, at doi:https://doi.org/10.1016/j.mex.2019.11.015.

References

[1] G. Renner, T.C. Schmidt, J. Schram, Analytical methodologies for monitoring micro(nano)plastics: which are fit for purpose? Curr. Opin. Environ. Sci. Health 1 (2018) 55–61, doi:http://dx.doi.org/10.1016/j.coesh.2017.11.001.
[2] J. Li, H. Liu, J.P. Chen, Microplastics in freshwater systems: a review on occurrence, environmental effects, and methods for microplastics detection, Water Res. 137 (2018) 362–374, doi:http://dx.doi.org/10.1016/j.watres.2017.12.056.
[3] H.K. Imhof, J. Schmid, R. Niessner, N.P. Ivleva, C. Laforsch, A novel, highly efficient method for the separation and quantification of plastic particles in sediments of aquatic environments, Limnol. Oceanogr. Methods 10 (7) (2012) 524–537, doi:http://dx.doi.org/10.4319/lom.2012.10.524.
[4] M.G.J. Löder, H.K. Imhof, M. Ladehoff, L.A. Löschel, C. Lorenz, S. Mintenig, S. Piehl, S. Primpke, I. Schrank, C. Laforsch, G. Gerdts, Enzymatic purification of microplastics in environmental samples, Environ. Sci. Technol. 51 (24) (2017) 14283–14292, doi:http://dx.doi.org/10.1021/acs.est.7b03055.
[5] M.-T. Nuelle, J.H. Dekiff, D. Remy, E. Fries, A new analytical approach for monitoring microplastics in marine sediments, Environ. Pollut. 184 (2014) 161–169, doi:http://dx.doi.org/10.1016/j.envpol.2013.07.027.
[6] J. Wagner, Z.-M. Wang, S. Ghosal, C. Rochman, M. Gassel, S. Wall, Novel method for the extraction and identification of microplastics in ocean trawl and fish gut matrices, Anal. Methods 9 (9) (2017) 1479–1490, doi:http://dx.doi.org/10.1039/c6ay02396g.
[7] L. Zada, H.A. Leslie, A.D. Vethaak, G.H. Tinnevelt, J.J. Jansen, J.F. de Boer, F. Ariese, Fast microplastics identification with stimulated raman scattering microscopy, J. Raman Spectrosc. 49 (7) (2018) 1136–1144, doi:http://dx.doi.org/10.1002/jrs.5367.

[8] B.E. Oßmann, G. Sarau, S.W. Schmitt, H. Holtmannspötter, S.H. Christiansen, W. Dicke, Development of an optimal filter substrate for the identification of small microplastic particles in food by micro-raman spectroscopy, Anal. Bioanal.Chem. 409 (16) (2017) 4099–4109, doi:http://dx.doi.org/10.1007/s00216-017-0358-y.
[9] N.P. Ivleva, A.C. Wiesheu, R. Niessner, Microplastic in aquatic ecosystems, Angew. Chem. Int. Ed. 56 (7) (2016) 1720–1739, doi:http://dx.doi.org/10.1002/anie.201606957.
[10] J.C. Prata, J.P. da Costa, A.C. Duarte, T. Rocha-Santos, Methods for sampling and detection of microplastics in water and sediment: a critical review, TrAC Trends Anal. Chem. 110 (2019) 150–159, doi:http://dx.doi.org/10.1016/j.trac.2018.10.029.
[11] S. Primpke, C. Lorenz, R. Rascher-Friesenhausen, G. Gerdts, An automated approach for microplastics analysis using focal plane array (FPA) FTIR microscopy and image analysis, Anal. Methods 9 (9) (2017) 1499–1511, doi:http://dx.doi.org/10.1039/c6ay02476a.
[12] M.G.J. Löder, M. Kuczera, S. Mintenig, C. Lorenz, G. Gerdts, Focal plane array detector-based micro-fourier- transform infrared imaging for the analysis of microplastics in environmental samples, Environ. Chem. 12 (5) (2015) 563, doi:http://dx.doi.org/10.1071/en14205.
[13] A. Käppler, D. Fischer, S. Oberbeckmann, G. Schernewski, M. Labrenz, K.-J. Eichhorn, B. Voit, Analysis of environmental microplastics by vibrational microspectroscopy: FTIR, raman or both? Anal. Bioanal. Chem. 408 (29) (2016) 8377–8391, doi:http://dx.doi.org/10.1007/s00216-016-9956-3.
[14] I.W. Levin, R. Bhargava, Fourier transform infrared vibrational spectroscopic imaging: integrating microscopy and molecular recognition, Annu. Rev. Phys. Chem. 56 (1) (2005) 429–474, doi:http://dx.doi.org/10.1146/annurev.physchem.56.092503.141205.
[15] T. Maes, R. Jessop, N. Wellner, K. Haupt, A.G. Mayes, A rapid-screening approach to detect and quantify mi- croplastics based on fluorescent tagging with nile red, Sci. Rep. 7 (March (1)) (2017), doi:http://dx.doi.org/10.1038/srep44501.
[16] D. Schymanski, C. Goldbeck, H.-U. Humpf, P. Fürst, Analysis of microplastics in water by micro-raman spectroscopy: release of plastic particles from different packaging into mineral water, Water Res. 129 (2018) 154–162, doi:http://dx.doi.org/10.1016/j.watres.2017.11.011.
[17] S. Huppertsberg, T.P. Knepper, Instrumental analysis of microplastics—benefits and challenges, Anal. Bioanal. Chem. 410 (25) (2018) 6343–6352, doi:http://dx.doi.org/10.1007/s00216-018-1210-8.
[18] G. Renner, T.C. Schmidt, J. Schram, A new chemometric approach for automatic identification of microplastics from environmental compartments based on FT-IR spectroscopy, Anal. Chem. 89 (22) (2017) 12045–12053, doi:http://dx.doi.org/10.1021/acs.analchem.7b02472.
[19] G. Renner, P. Sauerbier, T.C. Schmidt, J. Schram, Robust automatic identification of microplastics in environmental samples using FTIR microscopy, Anal. Chem. 91 (15) (2019) 9656–9664, doi:http://dx.doi.org/10.1021/acs.analchem.9b01095c.
[20] A. Murray, S. Landey, Pillow URL, (2015) . https://github.com/python-pillow/Pillow/blob/3.1.x/docs/reference/ImageGrab.rst.
[21] M. Hammond, Pywin32 URL, (2018) . https://github.com/mhammond/pywin32.
[22] S. Hoffstaetter, J. Bochi, M. Lee, L. Kistner, R. Mitchell, E. Cecchini, Python-Tesseract URL, (2019) . https://pypi.org/project/pytesseract/.
[23] K. Abid Rahman, Opencv2-Python-Tutorials URL, (2013) . https://github.com/abidrahmank/OpenCV2-Python-Tutorials/blob/master/source/py_tutorials/py_imgproc/py_watershed/py_watershed.rst.
[24] E. Olson, Particle shape factors and their use in image analysis part 1: theory, J. GXP Compliance 15 (3) (2011) 85.
[25] ISO 9276-6: Descriptive and Quantitative Representation of Particle Shape and Morphology, Standard, International Organization for Standardization, Geneva, CH, 2008 Mar..